# Plasmonically Amplified Fluorescence Bioassay with Microarray Format

S. Gogalic[a], S. Hageneder[b], C. Ctortecka[b], M. Bauch[b,c], I. Khan[b,c], C. Preininger[a], U. Sauer[a], J. Dostalek[b*]

[a]Bioresources, Health and Environment Department, AIT-Austrian Institute of Technology, Konrad Lorenz Strasse 24, 3430 Tulln, Austria; [b]Biosensor Technologies, AIT-Austrian Institute of Technology, Muthgasse 11, 1190 Vienna, Austria, [c]Energy Department, AIT-Austrian Institute of Technology, Giefinggasse 2, 1210 Vienna, Austria

## ABSTRACT

Plasmonic amplification of fluorescence signal in bioassays with microarray detection format is reported. A crossed relief diffraction grating was designed to couple an excitation laser beam to surface plasmons at the wavelength overlapping with the absorption and emission bands of fluorophore Dy647 that was used as a label. The surface of periodically corrugated sensor chip was coated with surface plasmon-supporting gold layer and a thin SU8 polymer film carrying epoxy groups. These groups were employed for the covalent immobilization of capture antibodies at arrays of spots. The plasmonic amplification of fluorescence signal on the developed microarray chip was tested by using interleukin 8 sandwich immunoassay. The readout was performed *ex situ* after drying the chip by using a commercial scanner with high numerical aperture collecting lens. Obtained results reveal the enhancement of fluorescence signal by a factor of 5 when compared to a regular glass chip.

**Keywords:** fluorescence, plasmonics, microarrays, bioassay, diffraction grating

## 1. INTRODUCTION

Fluorescence microarrays represent an established technology that is routinely used in important areas of life sciences, medical diagnostics, and food safety [1, 2] for highly parallelized detection of nucleic acid and protein analytes. In these applications, ligands are typically immobilized at arrays of spots on a glass sensor chip and incubated with analyzed liquid sample in order to specifically bind target analytes. The amount of captured analyte is detected by using fluorophore labels. The majority of fluorescence microarray scanners rely on epi-fluorescence geometry in which fluorescence signal from individual spots is detected *ex situ* by scanning an excitation laser beam across the microarray. In order to analyze smaller amounts of captured analyte at a sensing spot, an integration of various optical structures to sensor chips was proposed for increasing the detected fluorescence intensity per attached fluorophore label. These include multilayer dielectric structures that serve as a Bragg mirror for improving the extraction of fluorescence light from the chip. This approach prevents leaking of fluorescence light into the glass substrate (in form of supercritical angular fluorescence – SAF [3]) [4, 5]. In addition, laterally structured dielectric multi-layers were explored for the fluorescence enhancement through diffraction coupling of light to waveguide modes [6] and Bloch surface waves [7] that interact with fluorophores via their near field.

Besides dielectric structures, the employment of metallic nanostructures gained increasing interest for the enhancement of fluorescence assays owing to their unique plasmonic properties [8]. The coupling of fluorophore labels with plasmonic metallic nanostructures offers efficient means for the fluorescence signal amplification [9, 10] which can reach a factor as high as $10^3$ [11] for individual molecules placed at so-called "plasmonic hotspots". By using diffraction on periodically corrugated metallic grating, the far field electromagnetic radiation can excite surface plasmons (SPs) that travel along a metal surface and originate from collective oscillations of electron density. SPs exhibit much tighter confinement of the electromagnetic field intensity than dielectric waveguide modes and thus they stronger interact with fluorophores. The emitted fluorescence light intensity from fluorophores exposed to surface plasmon field can be particularly increased by the combination of two effects: by increasing the excitation rate with SP-enhanced intensity at the fluorophore absorption wavelength $\lambda_{ab}$ and by the directional SP-coupled emission at emission wavelength $\lambda_{em}$ that allows for higher yield in the fluorescence light detection. Due to the strongly confined SP-field, the amplification of fluorescence signal occurs at only small proximity to the metallic surface (*e.g.*, the probing depth of propagating surface

Optical Sensors 2015, edited by Francesco Baldini, Jiri Homola, Robert A. Lieberman, Proc. of SPIE
Vol. 9506, 95060N · © 2015 SPIE · CCC code: 0277-786X/15/$18 · doi: 10.1117/12.2179470

plasmons on a continuous gold surface in the red part of spectrum is of about $L_p$~100 nm). The grating coupled SP-enhanced fluorescence is ideally suited for *in situ* epi-fluorescence detection of fluorescence signal which relies on relatively low numerical aperture lens and can provide the enhancement factor of about $10^2$. This enhancement can translate to increased sensitivity in assays [12, 13] as well as it allows fluorescence observation of molecular binding kinetics [14] which is otherwise masked by strong background signal originating from the bulk solution.

This paper reports an implementation of plasmonic diffraction gratings to protein microarray chip with *ex situ* readout by a fluorescence scanner with epi-fluorescence geometry and high numerical aperture optics for the collecting of fluorescence light. Design of the structure is described and its performance characteristics are investigated by using interleukin 8 (IL-8) sandwich immunoassay. The need of compatibility of prepared plasmonic sensor chip with mass production technologies is addressed and an immobilization strategy of ligands that is identical with regularly used epoxy glass chips [15] is adopted.

## 2. MATERIALS AND METHODS

### Chemicals and Biochemicals

Positive photoresist Microposit S1805 was purchased from Shipley and its developer AZ 303 was acquired from MicroChemicals. Polydimethylsiloxane elastomer (PDMS) Sylgard 184 was obtained from Dow Corning and the UV-curable polymer Amonil MMS 110 was from AMO GmbH. SU8 resin (Epikote 157, batch 12XNG3) was from Micro Resist Technology and it was diluted by propylene glycol monomethyl ether acetate (PGMEA) from Sigma Aldrich (48,443-1, Lot: STBB2425). Affinity purified anti-human IL-8 (clone H8A5, 511501) and biotin-labeled anti-human IL-8 (clone E8N1, 511403) were purchased from Biozyme. Human IL-8 recombinant protein (14-8089-80) was from eBioscience and streptavidin labeled with Dy647 (dye similar to Cy5 with the absorption wavelength close to $\lambda_{ab}$=640 nm and emission band centered at the wavelength of $\lambda_{em}$=670 nm) was obtained from Dyomics (Germany). LowCross-Buffer (product number 100 050) from Candor was used in the assay experiments. Tween 20 and sodium deoxycholate were from Sigma.

### Preparation of plasmonic sensor chips

Crossed grating structure was recorded by UV laser interference lithography (LIL) with Lloyd's mirror configuration. Firstly, a BK7 glass substrate was coated with 400 nm thick photoresist Microposit S1805 layer by using spin-coating (4500 rpm for 45 seconds) and it was soft baked on a hot plate at 98 °C for 120 sec. Afterwards, the substrate was mounted to the LIL setup (see Figure 1a) with the angle of interfering expanded beams at a wavelength of $\lambda$=325 nm (with the intensity of 32 μW/cm$^2$ emitted from a HeCd laser IK 3031 R-C from Kimmon) set to $\theta$=15.65 deg. This angle was selected in order to record a structure with the period $\Lambda$=602.3 nm. The photoresist layer was exposed twice to the interference field for 60 seconds and the substrate was rotated by 90 deg between the first and seconds exposures. After the exposition, the crossed relief structure was etched into the photoresist by its immersing for $t$=25 sec in the developer AZ 303 that was diluted with distilled water at the ratio of 1:14.

From the relief master structure etched into the photoresist S1805, multiple copies were prepared by UV soft lithography as described by Figure 1b. Firstly, a PDMS working stamp was fabricated. The temperature upon which the PDMS was cured on the top of the master structure was controlled in the range of 30-50 °C in order to fine tune the period of the PDMS copy (the increasing of curing temperature from 30 °C to 50 °C was accompanied with a decrease of the grating period $\Lambda$ by about 5 nm due to difference in the thermal expansion of the master and PDMS). Afterwards, the cured PDMS working stamp was released from the master and used to prepare multiple copies of the corrugation. UV-curable polymer Amonil MMS 10 was spin-coated on a cleaned BK7 glass substrate at 2000 rpm for 120 s which results to a layer with a thickness of 110 nm. Then, the PDMS working stamp was placed on the top of the Amonil surface and irradiated by UV light (UV lamp Bio-Link 365, Vilber Lourmat) at $\lambda$=365 nm. The irradiation dose was 5 J/cm$^2$. Finally, the PDMS stamp was detached from the cured Amonil MMS 10 leaving a copy of the master structure. The Amonil replicas were subsequently coated with 4 nm of Cr and 100 nm of Au by vacuum thermal evaporation (HHV AUTO 306 from HHV LTD) in vacuum better than $10^{-6}$ mBar. It should be noted that prepared sample carried an area that was structured and an area that was flat and served as a reference in the further optical measurements.

On the gold surface, an SU8 polymer layer was spin-coated from a solution where SU8 was diluted with PGMEA to the concentration 0.5 %. This polymer layer served as a linker layer for subsequent spotting of antibodies for the capture of target analyte.

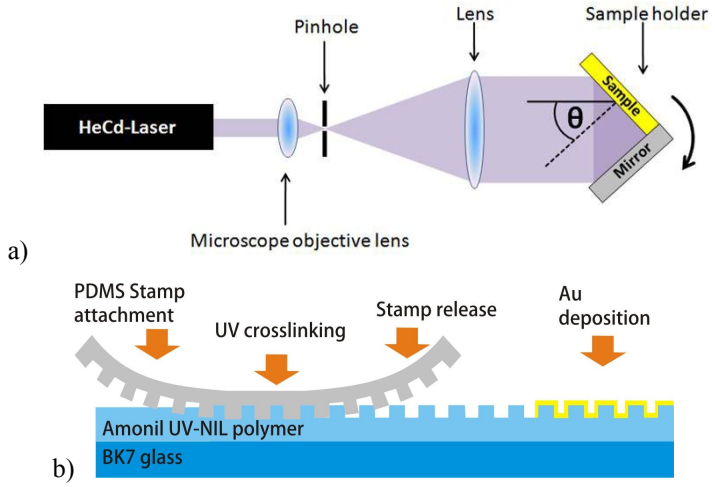


Figure 1. Schematics of a) laser interference lithography setup for the preparation of crossed relief grating master and b) the preparation of replicas for the plasmonic amplification of fluorescence signal by using soft lithography.

### Characterization of plasmonic sensor chip

In order to observe the resonant excitation of SP modes on prepared plasmonic chips, an in house-built optical system was employed for the measurement of angular – wavelength reflectivity spectra (for detailed description see our previous work [14]). The thickness of the SU8 layer and its modification with protein molecules was measured on a flat surface by using surface plasmon resonance (SPR) sensor with angular interrogation and the wavelength of 633 nm. This SPR sensor system was developed in house and it is described in our previous study [16]. The measured SPR angular scans were analyzed by software Winspall that was developed at the Max Plank Institute for Polymer Research (MPIP, Mainz, Germany). The grating morphology was observed with atomic force microscopy (AFM) Nano Wizard II from JPK instruments.

### Bioassay detection format

Affinity purified anti-human IL-8 (capture antibody - cAb) was diluted in a printing phosphate buffered saline (PBS with 0.01% sodium deoxycholate, pH 7.2) at a concentration of 0.4 mg/mL and spotted on the sensor chip surface. The optimum spotting conditions (composition of print buffer, humidity during spotting and antibody concentration) were established based on our previous research [17]. The cAb was arrayed on the plasmonic chips with SU8 layer or on ARChip Epoxy slides with identical SU8 polymer. The Omnigrid contact spotter with SMP3 pin from GeneMachines was used and operated at a relative humidity of 50 %. The spot-to-spot distance was set to 350 µm and the diameter of each spot was set to around 100 µm. Each chip carried three rows of spots that served a) for detection of IL8 (the cAb was spotted), b) as a control (blank printing buffer was spotted), and c) as a lead (IgG antibody against another analyte with attached Dy647 dye was spotted). In order to maximize the binding capacity of cAb spots, the printed slides were stored at 4 °C for at least three days. After the spotting, blocking of the surface outside the microarray spots was performed by the incubation in PBS spiked with 0.1% Tween 20 for 30 min. This step allowed for removing loosely bound molecules from the spots and for the deactivation of non-reacted epoxy surface groups. Finally, the slides were washed two times with PBS (pH 7.2) and dried by compressed air.

As Figure 2 shows, sandwich immnoassay was used for the detection of IL-8 analyte. As a sample, the assay buffer was spiked with IL-8 at the concentration 27 pg/mL. Microarrays on the plasmonic sensor chip and ARChip Epoxy slides were incubated with 50 µL of the sample for 2.5 h. Afterwards, the surface was washed three times by PBS with 0.1%

Tween-20 and incubated for 45 min with 50 µL of biotin-labeled anti-human IL-8 (detection antibody - dAb) diluted at the concentration of 1 µg/mL. Then, the surface was washed again three times by PBS with 0.1% Tween 20 and incubated with 4 µg/mL Dy647 streptavidin for 45 min. Finally, each slide was washed twice by PBS with 0.1% Tween 20 and twice in PBS, dried by using compressed air, and stored in the dark until scanning.

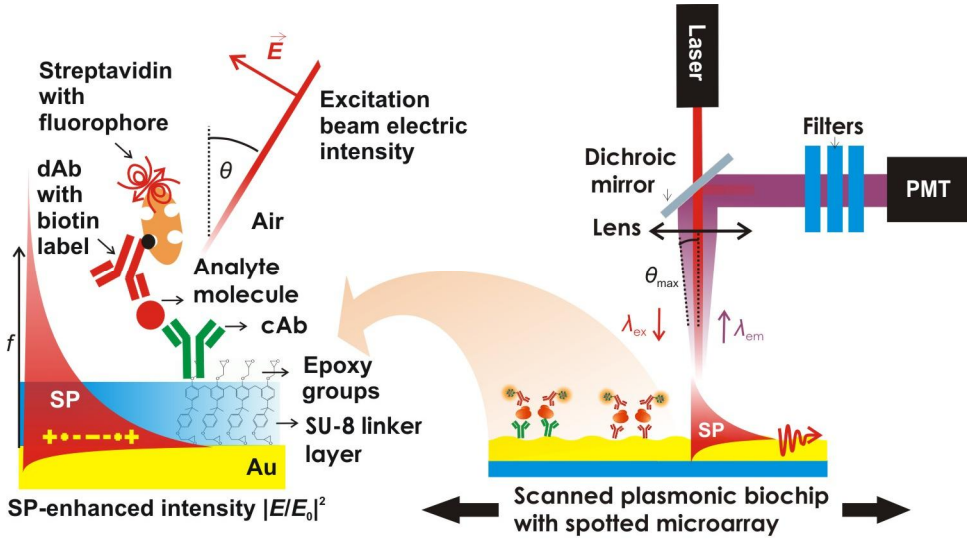


Figure 2. Schematics of prepared sensor chip for epi-fluorescence detection with an interface architecture for sandwich assay detection format.

### Fluorescence microarray readout

For the readout of microarray assay on the plasmonic and ARChip Epoxy slides, Genepix 4000B microarray fluorescence scanner (from Axon Instruments, USA) was used. The measurement utilized an epi-fluorescence readout geometry (see Figure 2) where an excitation laser beam at the wavelength of $\lambda_{ex}$=635 nm is focused at the surface by using a lens with a numerical aperture $NA$=0.68 in order to excite fluorophore labels attached to the sensor chip. The same lens is used for the collecting of the emitted fluorescence light beam at emission wavelength $\lambda_{em}$~670 nm that is delivered to photomultiplier tube (PMT) operated at constant voltage through all experiments. In the optical system of the scanner, the excitation beam is blocked by using a dichroic mirror and a set of fluorescence filters. The numerical aperture $NA$ of the lens used for the collecting of emitted fluorescence light translates to the maximum acceptance polar angle of $\theta_{max}$=43 deg (see Figure 2). Obtained fluorescence data were analyzed with the Genepix 6.0 software. The mean signal values were calculated from ten background corrected data points. Data that were out of the mean signal values ± the standard deviation (SD) were excluded.

## 3. RESULTS AND DISCUSSION

### Spectrum of diffraction-coupled surface plasmon modes

As illustrated in Figure 3, the prepared plasmonic chips carry a crossed grating with two superimposed orthogonal periodic corrugations in the $x$ and $y$ directions. As observed by AFM presented in Figure 3a, the period of superimposed corrugations was of $\Lambda$=602 nm and it was set for the diffraction excitation of SPs via the grating vector parallel to $x$ axis [diffraction order (±1,0)] and $y$ axis [diffraction order (0,±1)] at a wavelengths close the $\lambda_{ab}$ and $\lambda_{em}$ of used Dy647 dye. When coated with Au, the diffraction on the grating allows for the phase-matching of a light beam propagating above the metal surface and SPs travelling along the metal interfaces. The interaction strength between these waves can be controlled by the modulation depth. The prepared samples exhibited rather shallow modulation depth of around 70 nm which corresponds to small increase in the area of the surface area by only several percent. For the immobilization of

cAb, the SU8 layer was spun on the Au plasmonic chips. Its thickness was adjusted to around $t_{SU8}$=12 nm in order to assure that the fluorophore label is far enough from the Au surface in order to prevent quenching due to the Förster energy transfer. Let us note that the thickness of identical SU8 polymer on ARChip Epoxy glass substrate was much higher as the film was prepared by dip coating.

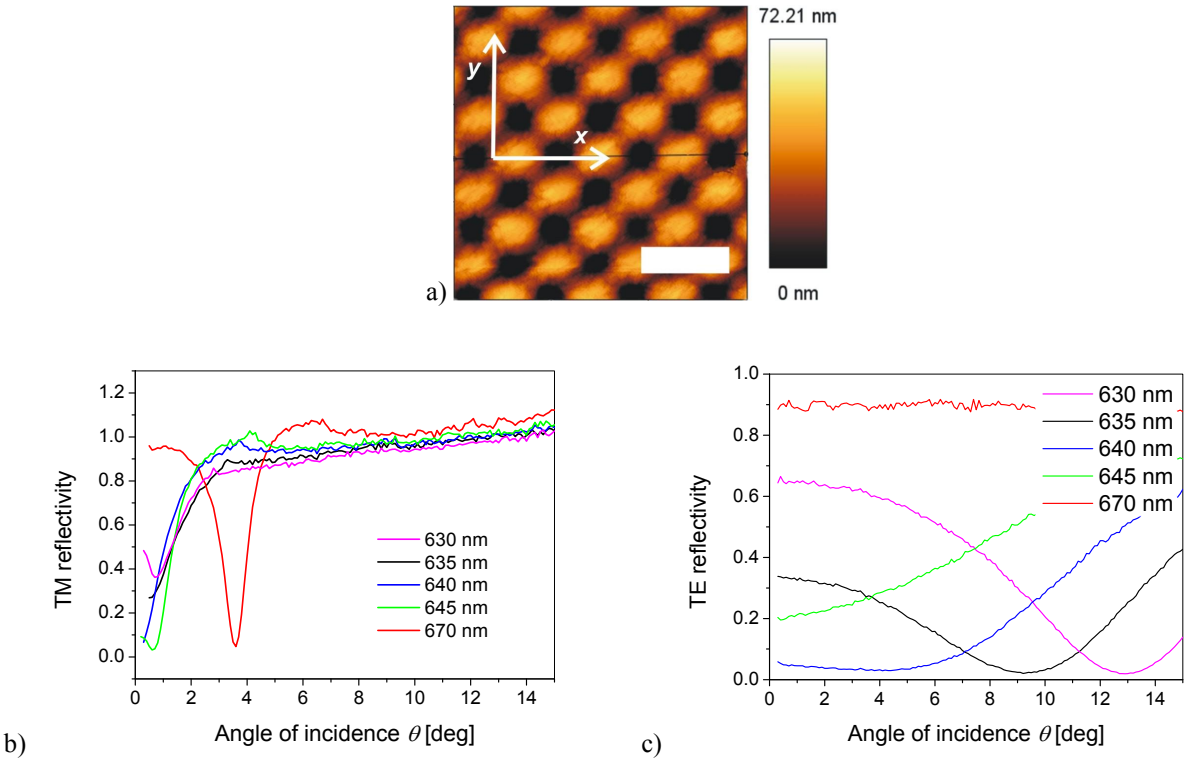


Figure 3. AFM characterization of grating morphology (a scale bar length of 0.6 μm) and b) TM and c) TE angular reflectivity spectrum for the prepared plasmonic chip with the SU8 layer coating (thickness $t_{SU8}$=12 nm).

In order to employ the SP-enhanced field intensity for increasing the fluorescence excitation rate, the resonant excitation of SPs was tuned to occur at $\lambda_{ex}$ for polar angles $\theta$ close to the normal incidence. The data in Figure 3b and c show the SPR reflectivity spectra that were measured in vicinity to this wavelength at polar angles $\theta$=0-15 deg with the plane of incidence parallel to the $x$ axis. It reveals that SPR manifests itself as a reflectivity drop in the measured transversal electric (TE) and transversal magnetic (TM) spectrum. For the TM polarized light, SPR occurs for the wavelengths $\lambda$ between 630 and 640 nm at polar angles $\theta$ below 2 deg due to the coupling via the grating vector in the plane of incidence [diffraction order (±1,0)]. The angular dependence of TE reflectivity shows much broader SPR resonance in angular spectrum. It occurs at angles $\theta$ below ~ 15 deg and it is associated with the coupling via grating vector perpendicular to the plane of incidence [diffraction order (0,±1)]. Let us note that the excitation wavelength and polar angles of incidence of used scanner falls into this range. In addition, Figures 3b and c illustrate that the prepared plasmonic grating allows for the coupling of more than 95 per cent of incident light energy to SPs at the resonant angle for wavelength > 640 nm. For the smaller wavelengths the coupling strength slightly decreases due to the fact that the corrugation profile is not precisely sinusoidal and a bandgap opens in the surface plasmon dispersion relation [18].

At the emission wavelength $\lambda_{em}$=670 nm of the used fluorophore Dy647, the measured TM reflectivity spectrum reveals that the SPR occurs at around 4 deg. This assures that the surface plasmon-coupled emission at $\lambda_{em}$ will be re-emitted from the surface via the first order diffraction at this angle when SPs are propagating parallel to a grating vector ($x$ or $y$ direction) as investigated in our previous study [14]. The emission polar angle $\theta$ increases above 4 deg for SPs propagating at the direction deviated from the grating vectors.

**Fluorescence amplification of signal on prepared microarrays**

Figure 4 confirms that both plasmonic and ARChip Epoxy surfaces allowed for attaching protein molecules as seen in the lead array (yellow marked) with spots where Dy647-labeled IgG antibody was directly spotted. The other two sections on the chips represent arrays of spots that carry cAb against IL-8 (blue-marked measuring spots) and blank area (green-marked control spots). The aquired images after the assaying a sample with IL-8 concentration of 27 pg/mL reveal that the measuring array exhibits bright spots due to the subsequent binding of biotinylated dAb and Dy647-labeled streptavidin to the analyte captured by cAb. The comparison of the response on the blank spots (associated with the unspecific sorption of dAb and Dy647-labeled streptavidin) and measuring spots (associated with the specific analyte capture) reveal that the *ex situ* response on the plasmonic chip is about 5 times higher than that on the ARChip Epoxy. However, this enhancement is about a 20-times smaller than that observed in our previous study where similar plasmonic grating (with a period $\Lambda$=434 nm [14]) was used for *in situ* fluorescence assay directly in liquid samples. The reason is that the used microarray scanner for *ex situ* measurement utilizes a lens with much higher numerical aperture (NA=0.68) than that used for the previous *in situ* experiments (NA=0.2). Therefore, the range of polar angles $\theta$ at which the fluorescence light is excited and collected is much wider which leads to the following two effects. Firstly, substantial part of the incident light intensity at $\lambda_{ex}$ is not coupled to SPs as the resonance become detuned when the focused excitation beam hits the surface at polar angles of incidence $\theta > 2$ deg. This leads to the decreased descreased coupling efficiency to SPs that is associated with lower average field intensity enhacement $|E/E_0|^2$ and weaker excitation rate at $\lambda_{ab}$. In addition, the directional emission the confines the emitted fluorescence light in a cone with small polar angle does not change significantly the overall yield in the delivering of emitted photons to the PMT detector. Rather, it only leads to re-distribution of the emitted intensity within the acceptance cone defined by polar angles $\theta$=0-$\theta_m$.

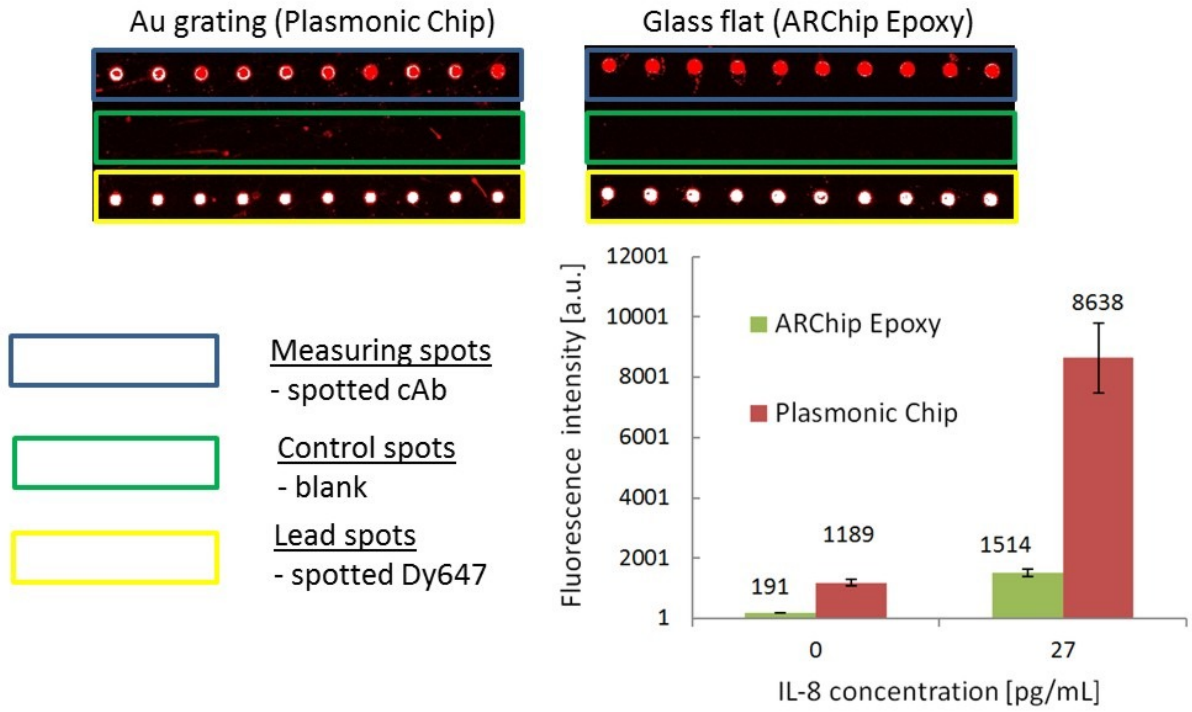


Figure 4. Example of fluorescence images for IL8 assay on microarrays spotted on developed Au grating (plasmonic chip) and regular (ARChip Epoxy) slides with measuring, control and lead arrays of spots (upper part). Comparison of fluorescence signal for the IL-8 assay is showed at the bottom.

## CONCLUSIONS

The implementation of plasmonic chip with crossed relief Au grating to fluorescence microarrays with *ex situ* detection format allowed for around 5-fold increased sensitivity as demonstrated by a model interleukin 8 sandwich assay. The preparation of selected nanostructure and the interface design for covalent immobilization of ligands was carried out by techniques that can be adopted for large scale fabrication. The study reveals that the plasmonic sensor chip utilizing diffraction coupling to propagating surface plasmons for the enhancement of fluorescence signal with *ex situ* detection is limited. The reason is the large numerical aperture optics for the excitation and collecting of fluorescence light which does not benefit from the highly directional surface plasmon-coupled emission and which lowers the excitation efficiency of surface plasmons. In particular, the plasmonic structure that would offer stronger amplification has to exploit the surface plasmon-assisted excitation of fluorescence light over broad range of angles of incidence. For such purpose, changing the shape of surface plasmon dispersion relation is possible and, for example, grating structures that support Bragg scattered surface plasmons [19] may be beneficial.

## ACKNOWLEDGMENT

This work was partially supported by the Austrian NANO Initiative (FFG and BMVIT) through the NILPlasmonics project within the NILAustria cluster (www.NILAustria.at), Austrian Science Fund (FWF) through the project PLASMOSOL (TRP-302), and FEMTECH – Frauen in Forschung und Technologie Initiative of the Austrian Ministry for Transportation, Innovation and Technology and FP7 Dipromon (no. 306157).

## REFERENCES

[1] M. Bally, M. Halter, J. Voros et al., "Optical microarray biosensing techniques," Surface and Interface Analysis, 38(11), 1442-1458 (2006).
[2] M. Seidel, and R. Niessner, "Automated analytical microarrays: a critical review," Analytical and Bioanalytical Chemistry, 391(5), 1521-1544 (2008).
[3] J. Enderlein, T. Ruckstuhl, and S. Seeger, "Highly efficient optical detection of surface-generated fluorescence," Applied Optics, 38(4), 724-732 (1999).
[4] H. Choumane, N. Ha, C. Nelep et al., "Double interference fluorescence enhancement from reflective slides: Application to bicolor microarrays," Applied Physics Letters, 87(3), (2005).
[5] M. Bras, V. Dugas, F. Bessueille et al., "Optimisation of a silicon/silicon dioxide substrate for a fluorescence DNA microarray," Biosensors & Bioelectronics, 20(4), 797-806 (2004).
[6] P. Karvinen, T. Nuutinen, O. Hyvarinen et al., "Enhancement of laser-induced fluorescence at 473 nm excitation with subwavelength resonant waveguide gratings," Optics Express, 16(21), 16364-16370 (2008).
[7] A. Angelini, E. Enrico, N. De Leo et al., "Fluorescence diffraction assisted by Bloch surface waves on a one-dimensional photonic crystal," New Journal of Physics, 15, (2013).
[8] J. A. Schuller, E. S. Barnard, W. S. Cai et al., "Plasmonics for extreme light concentration and manipulation," Nature Materials, 9(3), 193-204 (2010).
[9] M. Bauch, K. Toma, M. Toma et al., "Plasmon-Enhanced Fluorescence Biosensors: a Review," Plasmonics, 1-19 (2014).
[10] J. R. Lakowicz, K. Ray, M. Chowdhury et al., "Plasmon-controlled fluorescence: a new paradigm in fluorescence spectroscopy," Analyst, 133(10), 1308-1346 (2008).
[11] A. Kinkhabwala, Z. F. Yu, S. H. Fan et al., "Large single-molecule fluorescence enhancements produced by a bowtie nanoantenna," Nature Photonics, 3(11), 654-657 (2009).
[12] M. Tsuneyasu, C. Sasakawa, N. Naruishi et al., "Sensitive detection of interleukin-6 on a plasmonic chip by grating-coupled surface-plasmon-field-enhanced fluorescence imaging," Japanese Journal of Applied Physics, 53(6), (2014).
[13] K. Tawa, F. Kondo, C. Sasakawa et al., "Sensitive Detection of a Tumor Marker, α-fetoprotein (AFP), with a Sandwich Assay on a Plasmonic Chip," Analytical Chemistry, in press (2015).
[14] M. Bauch, S. Hageneder, and J. Dostalek, "Plasmonic amplification for bioassays with epi-fluorescence readout," Optics Express, 22(26), 32026-32038 (2014).

[15] C. Preininger, L. Bodrossy, U. Sauer et al., "ARChip Epoxy and ARChip UV for covalent on-chip immobilization of pmoA gene-specific oligonucleotides," Analytical Biochemistry, 330(1), 29-36 (2004).
[16] A. Aulasevich, R. F. Roskamp, U. Jonas et al., "Optical Waveguide Spectroscopy for the Investigation of Protein-Funcionalized Hydrogel Films," Macromolecular Rapid Communications, 30, 872-877 (2009).
[17] P. Domnanich, U. Sauer, J. Pultar et al., "Protein microarray for the analysis of human melanoma biomarkers," Sensors and Actuators B-Chemical, 139(1), 2-8 (2009).
[18] W. L. Barnes, T. W. Preist, S. C. Kitson et al., "Physical origin of photonic energy gaps in the propagation of surface plasmons on gratings," Physical Review B, 54(9), 6227-6244 (1996).
[19] M. Toma, K. Toma, P. Adam et al., "Surface plasmon-coupled emission on plasmonic Bragg gratings," Optics Express, 20(13), 14042-14053 (2012).